HETEROCYCLES, Vol. 83, No. 11, 2011, pp. 2563 - 2575. © 2011 The Japan Institute of Heterocyclic Chemistry
Received, 31st August, 2011, Accepted, 29th September, 2011, Published online, 5th October, 2011
DOI: 10.3987/COM-11-12352

CONFIRMATION OF MOLECULAR PLANARITY DISRUPTION EFFECT ON AQUEOUS SOLUBILITY IMPROVEMENT OF β-NAPHTHOFLAVONE ANALOGS

Yuji Fujita,[a] Mitsuhiro Yonehara,[a] Katsushi Kitahara,[b] Jun Shimokawa,[b] Yuichi Hashimoto,[a] and Minoru Ishikawa*,[a]

[a]Institute of Molecular and Cellular Biosciences, The University of Tokyo, 1-1-1 Yayoi, Bunkyo-ku, Tokyo 113-0032, Japan, [b]Graduate School of Pharmaceutical Sciences, University of Tokyo, 7-3-1 Hongo, Bunkyo-ku, Tokyo 113-0033, Japan
E-mail: m-ishikawa@iam.u-tokyo.ac.jp

Abstract – We have reported that increasing the dihedral angle of bicyclic molecules by ortho-substitution leads to increased aqueous solubility, which is extremely important for drug candidates. Here, we investigated in detail the improvement of aqueous solubility of β-naphthoflavone analogs by means of this approach as candidate aryl hydrocarbon receptor (AhR) agonists. To confirm the contribution of molecular planarity disruption to the increased solubility, we compared the effect of ortho-substitution with that of meta- or para-substitution with the same substituent. We also compared the wavelengths of maximum UV absorption to evaluate molecular planarity in solution, and determined the X-ray crystal structures to assess molecular planarity and crystal packing. The results support the idea that disruption of molecular planarity by substituent-induced increase of the dihedral angle results in a decrease of the crystal packing energy and a lower melting point, with a consequent increase of solubility.

INTRODUCTION

Aqueous solubility is essential for drug candidates. Poor aqueous solubility is likely to result in poor absorption, even if the permeation rate is high, since the flux of a drug across the intestinal membrane is proportional to the concentration gradient between the intestinal lumen and the blood. In addition, risk assessment of poorly soluble compounds is challenging, because exposure may be difficult to define and test sensitivity may be reduced. Further, high concentrations of poorly soluble drugs in organisms may

result in crystallization and acute toxicity. Overall, poor solubility of drug candidates has been identified as the cause of numerous drug development failures. Thus, it would be better to generate drug candidates with sufficient aqueous solubility at the drug discovery stage. Therefore, improvement of the aqueous solubility of bioactive molecules is a major and common issue in medicinal chemistry.[1] Decrease of log *P* by chemical modification, i.e., introduction of hydrophilic group(s) into molecules, is a classical and general strategy for improving aqueous solubility. But this approach is not universally effective.[1] Therefore, a novel and general strategy to increase the aqueous solubility of drug candidates would have a great impact on drug discovery and medicinal chemistry.

We have proposed an alternative strategy for improving aqueous solubility by means of disruption of molecular planarity and symmetry.[1] This strategy is based on the idea that the solubility of a solid solute in water is dependent on two factors: the crystallinity of the solute and the ability of the solute to interact with water.[2] Therefore, disruption of crystal packing is expected to improve aqueous solubility. We have focused on the modification of bicyclic lead molecules in ways that would disrupt molecular planarity by increasing the dihedral angle, or that would disrupt the molecular symmetry. By means of ortho-substitution of bicyclic molecules, we have generated integrin antagonists,[3-5] aryl hydrocarbon receptor (AhR) agonists[6] and peroxisome proliferator-activated receptor (PPAR)δ partial agonists[7] with greatly enhanced aqueous solubility. Our results indicate that disruption of molecular planarity is effective to increase aqueous solubility: a 350-fold improvement of aqueous solubility by disruption of molecular planarity, despite increased hydrophobicity, was achieved in one example.[7] To clarify the mechanisms of improvement of aqueous solubility, we examined the changes in physico-chemical properties of representative compounds, including CLogP (calculated log *P*), retention time on reversed-phase HPLC, calculated dihedral angle, and melting point. A larger calculated dihedral angle and lower melting point were associated with improved aqueous solubility compared with the parent compounds, despite increased hydrophobicity. It was concluded that disruption of molecular planarity by ortho-substitution resulted in decreased crystal packing energy, consequently increasing the solubility.

In that work, dihedral angle was estimated by means of density functional theory (DFT) calculations[8] (B3LYP/6-31G*). So, it remains desirable to further examine in detail the relationship between solubility and experimentally measured planarity. Here, we investigated in detail the improvement of aqueous solubility of β-naphthoflavone analogs as candidate AhR agonists by means of this approach, focusing on experimental confirmation of the relationship between molecular planarity and solubility. For this purpose, we compared the effect of ortho-methyl substitution with that of meta- or para-methyl substitution. We

also measured the wavelength of maximum UV absorption to examine molecular planarity in solution and determined the X-ray crystal structures to evaluate molecular planarity in the crystal and crystal packing.

RESULTS AND DISCUSSION

AhR is a ligand-dependent transcription factor that mediates the toxicity of dioxin.[9] AhR expression is ubiquitous in vertebrate cells, but the physiological role of AhR is not yet fully understood. Known AhR ligands possess limited solubility (especially in aqueous solution), which is a great drawback to the use of these ligands as tools for investigating the physiological role of AhR. Therefore, potent AhR ligands with improved solubility are required. We aimed to decrease the molecular planarity of β-naphthoflavone **1**, a potent AhR agonist, and introduced substituent(s) (**2**, **5**-**7**, **10**, **11**) at the ortho-position of the phenyl group (Table 1).[6] Among these compounds, the difluoro analog **7** had the best overall profile, being seven times more potent in terms of AhR-agonistic activity and three times more soluble than **1**. Calculation showed that ortho-substitution (**2**, **5** and **7**) disrupted the planarity by increasing the dihedral angle, leading to lower melting point and so increasing the solubility. However, the effects of meta- or para-substitution on aqueous solubility remain unclear. Therefore, we also examined the effect of methyl substitution at the meta- and para-positions of **1**. In addition, although we have already introduced methyl group(s), fluorine(s) and methoxy group at the ortho-position of **1**, the effects of other substituents remain interesting. Therefore, we also introduced chlorine(s) at the ortho-position of **1**.

Synthesis of the novel β-naphthoflavone analogs **3**, **4**, **8** and **9** is outlined in Scheme 1. The aldol reaction[6] with ketone **12** and substituted benzaldehydes afforded **13**-**16**, respectively. Compounds **13**-**16** were treated with DDQ[6] to give **3**, **4**, **8** and **9**, respectively in moderate yields.

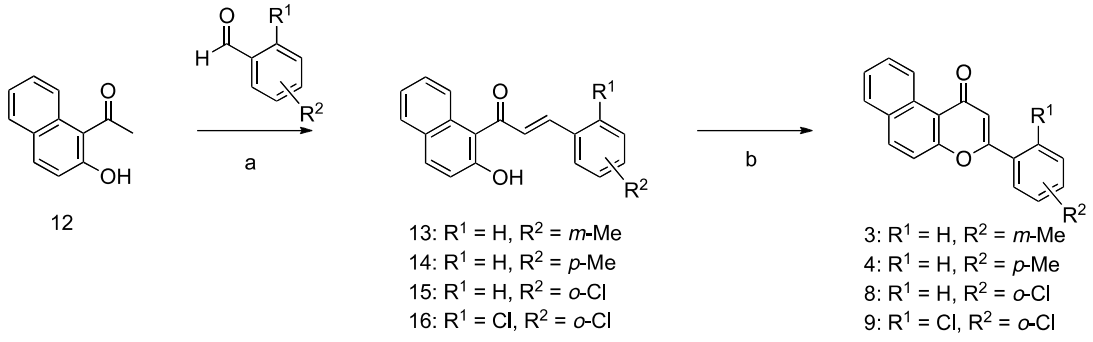

Scheme 1. Reagents and conditions: (a) NaOH, EtOH, H_2O, rt, (b) DDQ, 1,4-dioxane, 110 °C

Thermodynamic aqueous solubility (solubility of a compound as a saturated solution in equilibrium) of newly synthesized compounds was evaluated as previously reported.[6,7] The aqueous solubility of **1** in 1/15 M phosphate buffer (pH 7.4) was quite low (<0.15 μg/mL). So, a mixture of an equal volume of 1/15

M phosphate buffer (pH 7.4) and EtOH was used as an aqueous medium for the evaluation of thermodynamic solubility. To confirm the mechanism of the improved solubility of the biaryl analogs, physico-chemical parameters, that is, melting point, calculated dihedral angle, CLogP and retention time on reversed-phase HPLC, were evaluated. Dihedral angles in optimized structures of newly synthesized compounds were obtained by means of density functional theory (DFT) calculations (gas phase, B3LYP/6-31G*).[8] These physico-chemical properties of newly synthesized or previously reported β-naphthoflavone analogs are summarized in Table 1.

Table 1. AhR agonistic activity, solubility and physico-chemical properties of β-naphthoflavone analogs

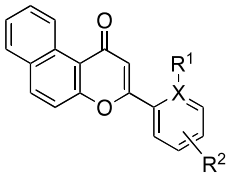

	R^1	R^2	X	EROD EC_{50} (μM)	solubility [a] (μg/mL)	melting point (°C)	calculated dihedral angle[b] (°)	λmax (nm)	CLogP[c]	HPLC retention time (min)[d]
1	H	H	C	1.4[e]	84.6[e]	165-167[e]	17.8[e]	273	4.7[e]	7.24
2	H	*o*-Me	C	>10[e]	262[e]	135-137[e]	37.9[e]	265	4.9[e]	8.17
3	H	*m*-Me	C	4.5	80.9	162	16.8	274	5.2	9.44
4	H	*p*-Me	C	2.8	35.4	194-195	16.5	285	5.2	9.43
5	Me	*o*-Me	C	>10[e]	1,270[e]	92[e]	70.0[e]	261	5.1[e]	9.13
6	F	H	C	0.33[e]	153[e]	157[e]	9.1[e]	270	4.8[e]	7.44
7	F	*o*-F	C	0.20[e]	248[e]	150[e]	40.5[e]	263	4.9[e]	7.44
8	H	*o*-Cl	C	>10	81.4	152	50.1	265	5.1	8.65
9	Cl	*o*-Cl	C	>10	150	160-161	79.7	261	5.6	10.7
10	OMe	H	C	0.27[e]	45.8[e]	192-193[e]	18.5[e]	272	4.1[e]	7.47
11	-	H	N	0.45[e]	299[e]	187-188[e]	0.0[e]	285	3.4[e]	4.52

[a] Solubility in an equal volume of EtOH and 1/15 M phosphate buffer (pH 7.4).

[b] Calculated dihedral angle was estimated with Gaussian03.

[c] CLogP values were estimated with ChemDraw Ultra version 10.0.

[d] Inertsil ODS-4 reversed-phase column (4.6 mm x 150 mm).

[e] Data taken from ref. 6.

Hydrophobicity parameters, CLogP and retention time on reversed-phase HPLC, indicate that the hydrophobicity of all monomethyl analogs (**2**, **3** and **4**) is increased, compared with that of non-substituted **1**. The order of calculated dihedral angle was ortho (**2**) ≫ non-substituted (**1**) ≧ meta (**3**)

≧ para (**4**), as expected. Furthermore, there was a relationship between aqueous solubility and melting point: the rank order of aqueous solubility (ortho (**2**) ≫ non-substituted (**1**) ≧ meta (**3**) > para (**4**)) corresponded to the order of melting points (ortho (**2**) ≪ meta (**3**) = non-substituted (**1**) < para (**4**)). Overall, the ortho-methyl analog **2** possesses the greatest solubility, the lowest melting point and the largest calculated dihedral angle among the four analogs. These results support our hypothesis that ortho-substitution disrupts molecular planarity by increasing the dihedral angle, leading in turn to lower melting point and so increasing the solubility. On the other hand, the meta-methyl analog **3** showed lower melting point and greater solubility than the para-methyl **4** analog. Thus, disruption of molecular symmetry by meta-substitution might also lead to decrease of melting point and increase of solubility.[1,7]

Next, we investigated the effect of ortho-chlorination. First, the values of CLogP and retention time on reversed-phase HPLC indicate that the hydrophobicity of the chloro analogs (**8** and **9**) is increased, depending on the number of chlorines introduced. The order of calculated dihedral angle was dichloro (**9**) > monochloro (**8**) > non-substituted (**1**), as expected. The melting point of monochloro analog **8** was lower than that of **1** indicating that a larger dihedral angle leads to less effective crystal packing of **8**. On the other hand, the melting point of dichloro analog **9** was higher than that of monochloro analog **8**. The reason for this is presumably that molecular weight, as well as crystal packing, influences melting point. The solubility of chloro analogs **8** and **9** was not increased as much as that of methyl analogs **2** and **5**: the order of solubility was dimethyl (**5**) > monomethyl (**2**) > dichloro (**9**) > non-substituted (**1**) ≧ monochloro (**8**). Possible reasons for lower solubility of the chloro analogs might be greater hydrophobicity and larger molecular weight. Still, comparison of dichloro analog **9** and non-substituted **1** suggests that the increase of dihedral angle did increase the solubility of **9**, even though the hydrophobicity was drastically increased.

To evaluate the AhR-agonistic activity, CYP1A1-dependent 7-ethoxyresorufin O-deethylase (EROD) activity[6] of MCF-7 breast cancer cells was measured. CYP1A1 is the major enzyme that catalyses the de-ethylation of 7-ethoxyresorufin to resorufin, and its activity is induced by activation of AhR. The activity of 7-ethoxyresorufin O-deethylase (EROD) can be measured by using fluorescent resorufin. The EROD activities of the newly synthesized compounds are shown in Table 1. Introduction of a methyl group in the meta (**3**) or para position (**4**) decreased the activity three-fold and two-fold compared with **1**, respectively. However, these compounds were more potent than ortho-methyl analog **2**. The EROD activities of the meta-methyl (**3**; dihedral angle: 16.8°) and para-methyl analogs (**4**; dihedral angle: 16.5°) were weaker than that of **1**, but stronger than that of the ortho-methyl analog (**2**; dihedral angle: 37.9°) suggesting that: 1) introduction of a methyl group decreases AhR agonistic activity, 2) a larger dihedral

angle is unfavorable for AhR agonistic activity. The chloro analogs **8** and **9** lacked EROD activity, indicating that their dihedral angle is too large or that the chlorine atom is too bulky.

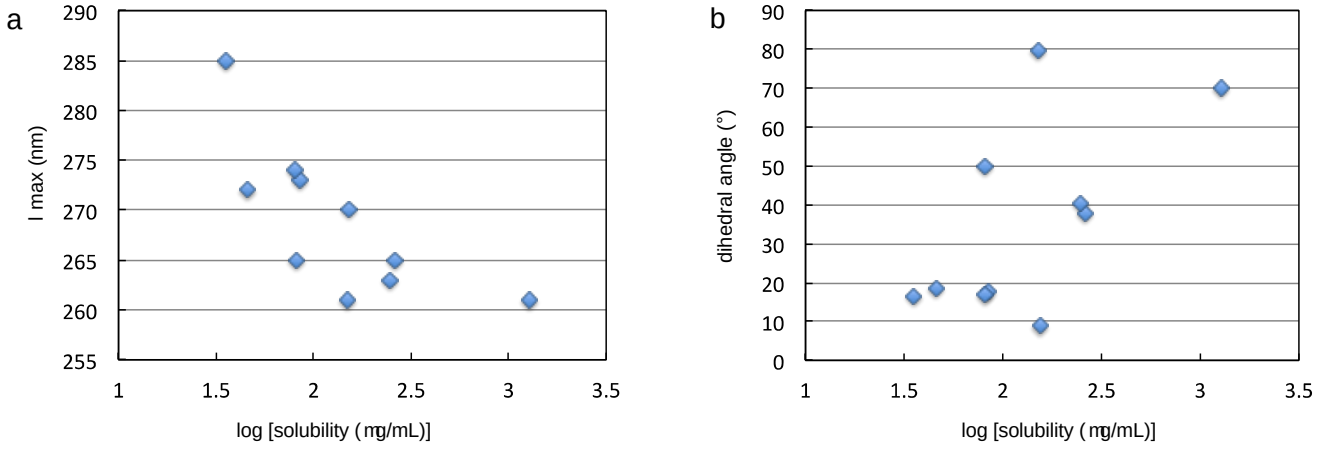

Figure 1. Relationships between solubility and molecular planarity of **1**-**10**: (a) λmax; (b) calculated dihedral angle

Extended conjugation of organic compounds results in a longer wavelength of maximum UV absorption (λmax). Thus, compounds with similar conjugation should show a negative correlation of λmax and dihedral angle. Therefore, we evaluated λmax as a parameter of molecular planarity. The λmax values of eleven compounds in methanol solution are shown in Table 1. β-Naphthoflavone analogs possessing the shortest wavelength were dimethyl analog **5** and dichloro analog **9** (λmax = 261 nm), which possess the second largest and the largest calculated dihedral angle, respectively. The compounds showing the longest wavelength were para-methyl derivative **4** and pyridyl analog **11** (λmax = 285 nm), which possess the third smallest and the smallest calculated dihedral angle, respectively. On the other hand, although **6** possessed the second smallest calculated dihedral angle, **6** showed higher hydrophobicity, lower melting point, and improved aqueous solubility compared with **1**. A possible explanation of the small calculated dihedral angle of **6** would be interaction between the fluorine lone pair and hydrogen at the 2-position.[6] However, the λmax value indicates that **6** possesses a larger dihedral angle than the planar analogs **1**, **10** and **11**. Analysis of eleven compounds showed that λmax was reasonably well correlated to calculated dihedral angle (R^2 = 0.67). We also plotted λmax and log (solubility) values, and calculated dihedral angle and log (solubility) values. Pyridyl analog **11**, a representative of the strategy of decreasing the hydrophobicity despite retaining a small dihedral angle,[6] was excluded from these plots. As shown in Figure 1, log(solubility) was more highly correlated with λmax (R^2 = 0.56) than with calculated dihedral angle (R^2 = 0.37). Thus, λmax might be useful parameter of molecular planarity, as well as calculated dihedral angle.

Finally, we performed single-crystal X-ray crystallographic analysis. Unfortunately, the crystal form of **1** was needle-shaped, which is not suitable for X-ray analysis. Therefore, we selected methoxy analog **10** as a representative compound with planar shape and low solubility. The reason for the relatively small calculated dihedral angle of **10** is presumably interaction between the oxygen lone pair and hydrogen at the 2-position.[6] We also selected dimethyl analog **5** as a representative compound with disruption of planarity and high solubility. The X-ray crystal structures of **5** and **10** are shown in Figure 2. The dihedral angle measured from the X-ray crystal structure of **5** is larger than that of **10** (Table 2). This result is consistent with the DFT calculations. Measured dihedral angle of **10** was larger than the calculated angle. Calculation in gas phase sometimes overestimates weak interaction might be one of the reasons. Next, the packing structures were analyzed. The crystal density of **5** obtained from the X-ray crystal structure is lower than that of **10**, indicating that the crystal packing energy of **5** is lower than that of **10**. All these data indicate that the increased solubility of **5** can be explained in terms of our hypothesis, that is, increase of dihedral angle results in disruption of molecular planarity, leading in turn to decreased crystal packing energy and lower melting point, and so increasing the solubility.

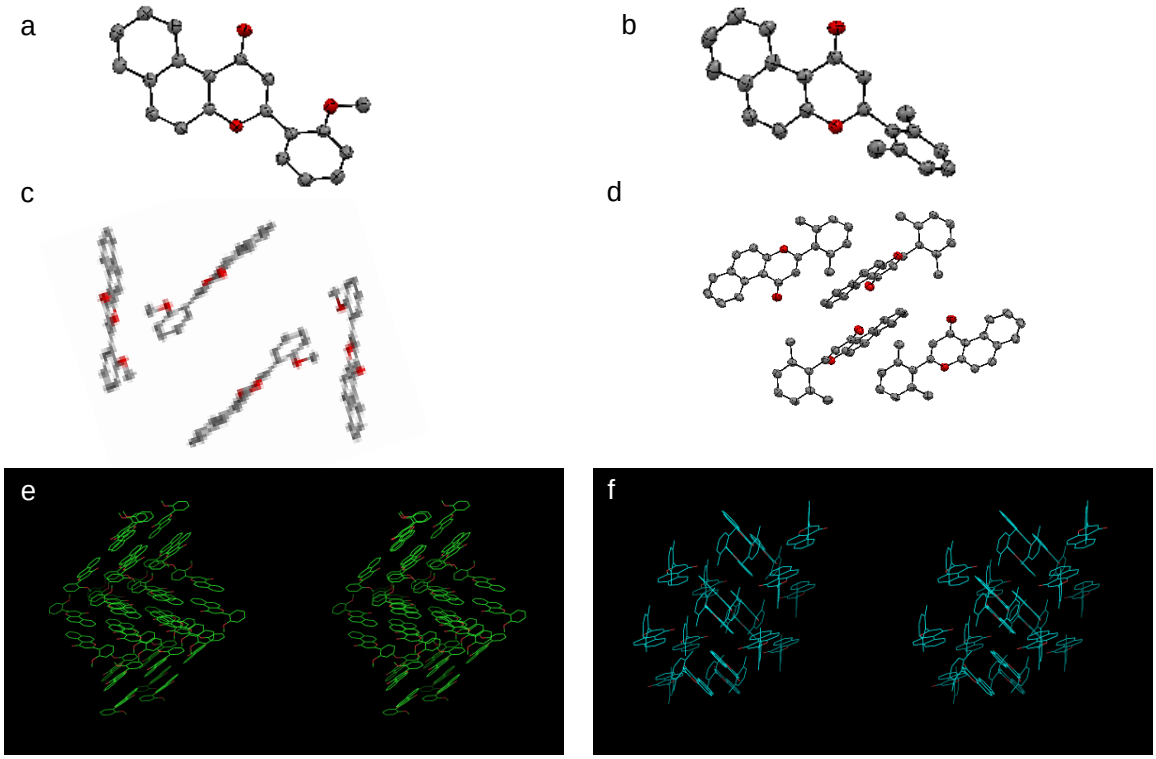

Figure 2. X-Ray crystal structures of **10** (a, c and e) and **5** (b, d and f). Single molecules are shown in a and b, packing structures in unit cells are shown in c and d, and stereo views of packing structures are shown in e and f

Table 2. Dihedral angle and crystal density obtained from X-ray crystallographic analysis of β-naphthoflavone analogs

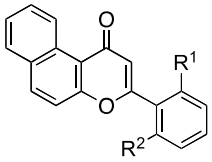

	R^1	R^2	solubility[a] (μg/mL)	measured dihedral angle (°)	calculated dihedral angle[b] (°)	crystal density (g/cm^3)	melting point (°C)	λmax (nm)
5	Me	*o*-Me	1270[c]	68.4	70.0[c]	1.301	92[c]	261
10	OMe	H	45.8[c]	31.1	18.5[c]	1.396	192-193[c]	272

[a] Solubility in an equal volume of EtOH and 1/15 M phosphate buffer (pH 7.4).

[b] Calculated dihedral angle was estimated with Gaussian03.

[c] Data taken from ref 6.

CONCLUSION

We have previously shown that increasing the dihedral angle by ortho-substitution of bicyclic molecules leads to increased solubility. Here, we investigated in detail the improvement of aqueous solubility of β-naphthoflavone analogs by means of this approach. We confirmed that ortho-methylation increased solubility, whereas meta- or para-methylation was ineffective. The λmax values of eleven compounds were correlated with calculated dihedral angle ($R^2 = 0.67$) and log (solubility) ($R^2 = 0.56$), indicating that λmax can be used as a parameter of molecular planarity. Finally, the X-ray crystallographically determined structures showed that more soluble **5** has an increased dihedral angle and decreased crystal density compared with less soluble **10**. All these results represent further evidence for the effectiveness of our strategy for improvement of aqueous solubility by disrupting molecular planarity.

EXPERIMENTAL

General methods

^{1}H NMR spectra were recorded on a JEOL JNMGX500 (500 MHz) spectrometer. Chemical shifts are expressed in parts per million relative to tetramethylsilane. Mass spectra were recorded on a JEOL JMS-DX303 spectrometer. Melting points were determined by using a Yanagimoto hot-stage melting point apparatus and are uncorrected. UV spectra were obtained in MeOH on a Shimadzu UV-2400PC spectrophotometer. Analytical thin-layer chromatography (TLC) was performed on Merck 60 F254 pre-coated silica gel plates. Flash chromatography was performed on a column of Kanto silica gel N 60.

HPLC analyses were performed on Inertsil ODS-4 reversed-phase column (5 μm, 4.6 mm x 150 mm) eluted with a mobile phase consisting of 1/30 M phosphate buffer (pH 7.4) in 70% MeCN at a flow rate of 1.0 mL/min, with UV monitoring at 258 - 288 nm, at 40 °C.

(*E*)-1-(2'-Hydroxynaphthalen-1'-yl)-3-(3"-methylphenyl)-2-propen-1-one (13).

To a solution of **12** (301 mg, 1.62 mmol) in EtOH (5 mL) was added a 3.3 M NaOH solution (5 mL). The resultant solution was cooled to 0 °C in an ice bath and 3-methylbenzaldehyde (0.230 mL, 1.95 mmol) was slowly added. The mixture was stirred at room temperature for 18 h, quenched with 1 M HCl solution and extracted with AcOEt. The organic layer was washed with brine, dried over $MgSO_4$, filtered, and concentrated. The residue was roughly purified by silica gel column chromatography (hexane/AcOEt = 20/1) to afford a mixture of **13** and **12** (249 mg) as an orange oil. The mixture was used in the next step without further purification.

^{1}H NMR (500 MHz, $CDCl_3$) δ 12.57 (s, 1H), 8.07 (d, *J* = 8.5 Hz, 1H), 7.93 (d, *J* = 8.5 Hz, 1H), 7.90 (d, *J* = 15.9 Hz, 1H), 7.82 (d, *J* = 7.9 Hz, 1H), 7.56-7.53 (m, 1H), 7.49 (d, *J* = 15.9 Hz, 1H), 7.45-7.41 (m, 3H), 7.32 (t, *J* = 7.9 Hz, 1H), 7.26-7.23 (m, 1H), 7.19 (d, *J* = 9.2 Hz, 1H), 2.39 (s, 3H); MS (FAB) m/z 288 $(M)^+$, 289 $(M+H)^+$.

Compounds **14**, **15**, and **16** were prepared using the same procedure as described for **13** from **12**.

(*E*)-1-(2'-Hydroxynaphthalen-1'-yl)-3-(4"-methylphenyl)-2-propen-1-one (14).

Compound **12** (306 mg, 1.64 mmol), 3.3 M NaOH solution (5 mL), and 4-methylbenzaldehyde (0.230 mL, 1.95 mmol) afforded a mixture of **14** and **12** (342 mg) as an orange oil. The mixture was used in the next step without further purification.

^{1}H NMR (500 MHz, $CDCl_3$) δ 12.58 (s, 1H), 8.07 (d, *J* = 6.7 Hz, 1H), 7.92 (d, *J* = 9.8 Hz, 1H), 7.91 (d, *J* = 15.9 Hz, 1H), 7.82 (d, *J* = 7.9 Hz, 1H), 7.55-7.52 (m, 3H), 7.47 (d, *J* = 15.9 Hz, 1H), 7.42-7.39 (m, 1H), 7.24 (d, *J* = 8.5 Hz, 2H), 7.19 (d, *J* = 9.2 Hz, 1H), 2.41 (s, 3H); MS (FAB) m/z 288 $(M)^+$, 289 $(M+H)^+$.

(*E*)-1-(2'-Hydroxynaphthalen-1'-yl)-3-(2"-chlorophenyl)-2-propen-1-one (15).

Compound **12** (306 mg, 1.64 mmol), 3.3 M NaOH solution (5 mL), and 2-chlorobenzaldehyde (0.220 mL, 1.95 mmol) afforded a mixture of **15** and **12** (249 mg) as an orange oil. The mixture was used in the next step without further purification.

MS (FAB) m/z 308 $(M)^+$, 309 $(M+H)^+$, 310 $(M+2)^+$, 311 $(M+3)^+$.

(*E*)-1-(2'-Hydroxynaphthalen-1'-yl)-3-(2",6"-dichlorophenyl)-2-propen-1-one (16).

Compound **12** (301 mg, 1.62 mmol), 3.3 M NaOH solution (5 mL), and 2,6-dichlorobenzaldehyde (352

mg, 2.01 mmol) afforded a mixture containing **16**. The mixture was purified by recrystallization from AcOEt/hexane to afford **12** (299 mg, 0.871 mmol, 54% yield) as an orange solid.

^{1}H NMR (500 MHz, $CDCl_3$) δ 12.68 (s, 1H), 8.14 (d, *J* = 7.9 Hz, 1H), 8.07 (d, *J* = 15.9 Hz, 1H), 7.94 (d, *J* = 8.5 Hz, 1H), 7.81 (d, *J* = 8.5 Hz, 1H), 7.65 (d, *J* = 15.9 Hz, 1H), 7.55-7.52 (m, 1H), 7.42-7.40 (m, 1H), 7.40 (d, *J* = 7.9 Hz, 2H), 7.26-7.22 (m, 1H), 7.20 (d, *J* = 9.2 Hz, 1H); MS (FAB) m/z 342 $(M)^+$, 343 $(M+H)^+$, 344 $(M+2)^+$, 345 $(M+3)^+$.

3-(3'-Methylphenyl)-1*H*-naphtho[2,1-*b*]pyran-1-one (3).

To a solution of a mixture of **13** and **12** (192 mg) in 1,4-dioxane was added DDQ (286 mg, 0.999 mmol), and the mixture was stirred at 110 °C for 3 h. Water was added, and the mixture was extracted with AcOEt. The organic layer was washed with brine, dried over $MgSO_4$, filtered, and concentrated. The residue was purified by means of silica gel column chromatography (hexane/AcOEt =10/1) to afford **3** (58.1 mg, 0.203 mmol, 23% yield in 2 steps) as a pale yellow solid. Compound **3** was crystallized from AcOEt/hexane.

Mp 162 °C. UV (MeOH) λmax (logε) 274 (4.48) nm. ^{1}H NMR (500 MHz, $CDCl_3$) δ 10.10 (d, *J* = 8.5 Hz, 1H), 8.13 (d, *J* = 9.2 Hz, 1H), 7.93 (d, *J* = 7.3 Hz, 1H), 7.79-7.76 (m, 3H), 7.66 (d, *J* = 8.5 Hz, 1H), 7.65-7.62 (m, 1H), 7.47-7.43 (m, 1H), 7.37 (d, *J* = 7.3 Hz, 1H), 6.98 (s, 1H), 2.49 (s, 3H); MS 286 $(M)^+$, 287 $(M+H)^+$. FAB-HRMS $(M+H)^+$ calcd for $C_{20}H_{15}O_2$: 287.1072, found: 287.1107. UV monitoring of HPLC at 275 nm.

Compounds **4**, **8**, and **9** were prepared using the same procedure as described for **3** from **13**.

3-(4'-Methylphenyl)-1*H*-naphtho[2,1-*b*]pyran-1-one (4).

DDQ (227 mg, 1.28 mmol) and a mixture of **14** and **12** (169 mg) afforded **4** (52.5 mg, 0.183 mmol, 23% yield in 2 steps) as a pale brown solid. Compound **4** was crystallized from AcOEt/hexane.

Mp 195-196 °C. UV (MeOH) λmax (logε) 285 (4.47) nm. ^{1}H NMR (500 MHz, $CDCl_3$) δ 10.10 (d, *J* = 8.5 Hz, 1H), 8.12 (d, *J* = 9.2 Hz, 1H), 7.93 (d, *J* = 7.9 Hz, 1H), 7.87 (d, *J* = 8.2 Hz, 2H), 7.79-7.76 (m, 1H), 7.65 (d, *J* = 9.2 Hz, 1H), 7.65-7.61 (m, 1H), 7.36 (d, *J* = 8.2 Hz, 2H), 6.96 (s, 1H), 2.46 (s, 3H); MS (FAB) m/z 286 $(M)^+$, 287 $(M+H)^+$. FAB-HRMS $(M+H)^+$ calcd for $C_{20}H_{15}O_2$: 287.1072, found: 287.1075.UV monitoring of HPLC at 282 nm.

3-(2'-Chlorophenyl)-1*H*-naphtho[2,1-*b*]pyran-1-one (8).

DDQ (328 mg, 1.44 mmol) and a mixture of **15** and **12** (227 mg) afforded **8** (90.1 mg, 0.294 mmol, 20% yield in 2 steps) as a pale yellow solid. Compound **8** was crystallized from AcOEt/hexane.

Mp 152 °C. UV (MeOH) λmax (logε) 265 (4.41) nm. ^{1}H NMR (500 MHz, $CDCl_3$) δ 10.09 (d, *J* = 8.5 Hz,

1H), 8.13 (d, *J* = 9.2 Hz, 1H), 7.93 (d, *J* = 8.5 Hz, 1H), 7.81-7.77 (m, 1H), 7.71 (dd, *J* = 7.9, 1.8 Hz, 1H), 7.66-7.63 (m, 1H), 7.58 (d, *J* = 9.2 Hz, 1H), 7.57 (dd, *J* = 7.9, 1.8 Hz, 1H), 7.48 (ddd, *J* = 7.3, 7.3, 1.8 Hz, 1H), 7.44 (ddd, *J* = 7.3, 7.3, 1.2 Hz, 1H), 6.86 (s, 1H); MS (FAB) m/z 306 $(M)^+$, 307 $(M+H)^+$, 308 $(M+2)^+$, 309 $(M+3)^+$. FAB-HRMS $(M+H)^+$ calcd for $C_{19}H_{12}ClO_2$: 307.0526, found: 307.0520. UV monitoring of HPLC at 267 nm.

3-(2',6'-Dichlorophenyl)-1*H*-naphtho[2,1-*b*]pyran-1-one (9).

Compound **16** (245 mg, 0.714 mmol) and DDQ (337 mg, 1.48 mmol) afforded **9** (158 mg, 0.463 mmol, 65% yield) as a pale yellow solid. Compound **9** was crystallized from AcOEt/hexane.

Mp 160-161 °C. UV (MeOH) λmax (logε) 261 (4.30) nm. ^{1}H NMR (500 MHz, $CDCl_3$) δ 10.09 (d, *J* = 8.5 Hz, 1H), 8.13 (d, *J* = 8.5 Hz, 1H), 7.94 (d, *J* = 7.9 Hz, 1H), 7.81-7.78 (m, 1H), 7.67-7.64 (m, 1H), 7.54 (d, *J* = 9.2 Hz, 1H), 7.49 (m, 2H), 7.43-7.40 (m, 1H), 6.63 (s, 1H); MS (FAB) m/z 340 $(M)^+$, 341 $(M+H)^+$, 342 $(M+2)^+$, 343 $(M+3)^+$. FAB-HRMS $(M+H)^+$ calcd for $C_{19}H_{11}Cl_2O_2$: 341.0136, found: 341.0155. UV monitoring of HPLC at 258 nm.

Thermodynamic aqueous solubility

The thermodynamic solubility was determined as reported previously.[6,7] Briefly, about 1 mg of compound was ground with an agate mortar and taken up in 1.0 mL of an equal volume of a mixture of 1:15 M phosphate buffer (pH 7.4) and EtOH. The suspension was shaken for 48 h at 25 °C. An aliquot was filtered through a Millipore DIMEX-13 (0.22 μm) or Millex-LG (0.20 μm) filter. The filtrate was diluted with DMF and injected into an HPLC with UV detection; peak areas were recorded at 258–295 nm. The concentration of the sample solution was calculated using a previously determined calibration curve, corrected for the dilution factor of the sample.

DFT Calculations

All calculations were performed at the DFT level, using the hybrid Becke3LYP (B3LYP) function as implemented in Gaussian 2003. The 6-31G* basis set was used for H, C, N, O and Cl atoms. Geometry optimization and vibrational analysis were performed at the same level. All stationary points were optimized without any symmetry assumptions and characterized by normal coordinate analysis at the same level of theory (number of imaginary frequencies, Nimag, 0).

UV absorption

1: (MeOH) λmax (logε) 273 (4.49) nm; **2**: (MeOH) λmax (logε) 265 (4.40) nm; **5**: (MeOH) λmax (logε) 261 (4.39) nm; **6**: (MeOH) λmax (logε) 270 (4.46) nm, **7**: (MeOH) λmax (logε) 263 (4.43) nm **10**:

(MeOH) λmax (logε) 272 (4.40) nm; **11**: (MeOH) λmax (logε) 285 (4.37) nm.

X-Ray crystallography

A colorless block crystals of **5** and **10** having appropriate dimensions was mounted on a glass filter. All measurements were made on a Rigaku RAXIS-IV imaging plate area detector with graphite monochromated Cu Kα radiation. Indexing was performed from three oscillations (exposure: 30 seconds). The data were collected at a temperature of -100±1 °C to a maximum 2θ value of 136.4°. A total of 60 or 45 (for **5** or **10**, respectively) oscillation images were collected. The crystal-to-detector distance was 127.40 mm with the detector at the zero swing position. Readout was performed in the 0.100 mm pixel mode. The structure was solved by direct methods[10] and expanded using Fourier techniques. Hydrogen atoms were refined using the riding model. The final cycle of full-matrix least-squares refinement on F was based on 2799 or 2631 (for **5** or **10**, respectively) observed reflections and 225 or 223 (for **5** or **10**, respectively) variable parameters, and converged.

Crystal data for **5**: $C_{21}H_{16}O_2$, FW 300.36, 0.15 x 0.14 x 0.11 mm, colorless crystal, monoclinic, a=8.3479(4) Å, b=13.5277(7) Å, c=13.9042(8) Å, b = 102.338(3)°, V = 1533.89(14) Å^3. CCDC-844361 contains the supplementary crystallographic data for this paper. These data can be obtained free of charge from the Cambridge Crystallographic Data Centre *via* www.ccdc.cam.ac.uk/data_request/cif.

Crystal data for **10**: $C_{20}H_{14}O_3$, FW 302.33, 0.17 x 0.10 x 0.17 mm, colorless crystal, monoclinic, a=7.4528(7) Å, b=22.457(2) Å, c=8.7772(9) Å, b = 101.757(5)°, V = 1438.2(2) Å^3. CCDC-844360 contains the supplementary crystallographic data for this paper. These data can be obtained free of charge from the Cambridge Crystallographic Data Centre *via* www.ccdc.cam.ac.uk/data_request/cif.

ACKNOWLEDGEMENTS

The work described in this paper was partially supported by Grants-in-Aid for Scientific Research from The Ministry of Education, Culture, Sports, Science and Technology, Japan, and the Japan Society for the Promotion of Science.

REFERENCES (AND NOTES)

1. M. Ishikawa and Y. Hashimoto, *J. Med. Chem.*, 2011, **54**, 1539.
2. N. Jain and S. H. Yalkowsky, *J. Pharm. Sci.*, 2001, **90**, 234.
3. M. Ishikawa, D. Kubota, M. Yamamoto, C. Kuroda, M. Iguchi, A. Koyanagi, S. Murakami, and K. Ajito, *Bioorg. Med. Chem.*, 2006, **14**, 2109.
4. M. Ishikawa, Y. Hiraiwa, D. Kubota, M. Tsushima, T. Watanabe, S. Murakami, S. Ouchi, and K. Ajito, *Bioorg. Med. Chem.*, 2006, **14**, 2131.

5. M. Ishikawa and K. Ajito, 'Soyaku Shien Kenkyu no Tenbo,' ed. by Y. Torisawa, CMC Publishing, Tokyo, 2008, pp. 3–13.
6. Y. Fujita, M. Yonehara, M. Tetsuhashi, T. Noguchi-Yachide, Y. Hashimoto, and M. Ishikawa, *Bioorg. Med. Chem.*, 2010, **18**, 1194.
7. J. Kasuga, M. Ishikawa, M. Yonehara, M. Makishima, Y. Hashimoto, and H. Miyachi, *Bioorg. Med. Chem.*, 2010, **18**, 7164.
8. All calculations were carried out with a GAUSSIAN 03 program package. GAUSSIAN 03, Revision E.01: Gaussian: Wallingford, CT, 2004.
9. M. S. Denison, A. Pandini, S. R. Nagy, E. P. Baldwin, and L. Bonati, *Chem. Biol. Interact.*, 2002, **141**, 3.
10. A. Altomare, M. Burla, M. Camalli, G. Cascarano, C. Giacovazzo, A. Guagliardi, A. Moliterni, G. Polidori, and R. Spagna, J. Appl. Cryst., 1999, 32, 115.